Control of Hairpin Formation via Proline Configuration in Parallel β-Sheet Model Systems

John D. Fisk,† Douglas R. Powell,‡ and Samuel H. Gellman*,†,‡

Contribution from the Graduate Program in Biophysics and Department of Chemistry, University of Wisconsin, Madison, Wisconsin 53706

Received August 16, 1999. Revised Manuscript Received January 29, 2000

Abstract: The simplest strategy for creation of parallel β-sheet model systems is to link adjacent peptide strands via their N-termini or via their C-termini. This connectivity requires unnatural linking segments. We describe dipeptide mimics that can serve as N-to-N or C-to-C linkers, and we demonstrate their efficacy by conformational analysis of tetrapeptide analogues in chloroform. The tetrapeptide analogues can adopt strand−loop−strand ("hairpin") conformations in which the residues at each end, L-valine and L-leucine, engage in parallel sheet hydrogen bonding interactions. Our linkers contain proline residues, to impart a preferred local twist. We show that linkers containing D-proline promote parallel sheet interactions between the strand L-residues, while linkers containing L-proline do not promote parallel sheet interactions. The preference for one linker twist is presumably related to the right-handed twist displayed by strands in protein β-sheets (parallel and antiparallel); analogous linker twist preferences have been observed in antiparallel β-sheet model systems.

Introduction

Elucidation of β-sheet folding preferences is crucial for understanding, predicting, and modifying native protein conformations.[1] It has recently become possible to design short peptides that display antiparallel β-sheet conformations in aqueous solution, and these model systems are beginning to provide fundamental insights on the noncovalent forces that influence antiparallel β-sheet stability.[2] Parallel β-sheet model systems are under development, with pioneering contributions from the laboratories of Nowick,[3] Kelly,[4] Kemp,[5] Feigel,[6] and others.[7] The simplest β-sheet models contain two peptide strand segments and a linking unit. For antiparallel juxtaposition of strands ("β-hairpin"), the linking segment can be composed of α-amino acids residues, but parallel strand juxtaposition requires a diamine or diacid linker. We report a study of proline-containing linkers for both N-to-N and C-to-C connection of peptide strands. Our results show that the proline configuration profoundly affects parallel sheet interactions between attached strand residues.

The experiments described here constitute a test of our hypothesis that parallel hairpin formation can be controlled via the local twist of the linker. This prediction arises from the observation that strands in parallel (and antiparallel) β-sheets in proteins display a right-handed twist.[8] Our hypothesis is a logical extrapolation from previous studies in which it was shown that antiparallel β-sheet formation between L-residue strands can be either promoted or discouraged with dipeptide linkers that contain either D-proline or L-proline, respectively.[9,10] We have now used proline to generate *parallel* linkers because proline is well-known to induce a reversal in backbone trajectory,[11,12] and because the rigidity conferred by the proline ring should allow the C_α configuration to exert a large effect on linker conformation.

Results and Discussion

Molecules **1** and **2** are analogues of a Pro-Xxx dipeptide. The prolyl-(1,1-dimethyl)-1,2-diaminoethyl core of **1** can link peptide strands via their C-termini, and the carbonyl-prolyl-glycyl core of **2** can link peptide strands via their N-termini. Urea-dipeptide **2** is related to linkers employed by Kemp et al., who used a carbonyl-L-prolyl-D-alanyl segment to connect a

* To whom correspondence should be addressed: gellman@chem.wisc.edu.
† Graduate Program in Biophysics.
‡ Department of Chemistry.

(1) Nesloney, C. L.; Kelly, J. W. *Bioorg. Med. Chem.* **1996**, *4*, 739.
(2) Gellman, S. H. *Curr. Opin. Chem. Biol.* **1998**, *2*, 717. Lacroix, E.; Kortemme, de la Paz, E. L.; Serranno, L. *Curr. Opin. Struct. Biol.* **1999**, *9*, 487.
(3) (a) Nowick, J. S.; Smith, E. M.; Noronha, G. *J. Org. Chem.* **1995**, *60*, 7386. (b) Nowick, J. S.; Insaf, S. *J. Am. Chem. Soc.* **1997**, *119*, 10903. (c) Nowick, J. S. *Acc. Chem. Res.* **1999**, *32*, 287.
(4) Chitnumsub, P.; Fiori, W. R.; Lashuel, H. A.; Diaz, H.; Kelly, J. W. *Bioorg. Med. Chem.* **1999**, *7*, 39.
(5) Kemp, D. S.; Blanchard, D. E.; Muendel, C. C. In *Peptides−Chemistry and Biology*; Smith, J., Rivier, J., Eds.; ESCOM: Leiden, 1992; p 319.
(6) Wagner, G.; Feigel, M. *Tetrahedron* **1993**, *49*, 10831.
(7) Winningham, M. J.; Sogah, D. Y. *Macromolecules* **1997**, *30*, 862. Skar, M. L.; Svendsen, J. S. *Tetrahedron* **1997**, *53*, 17425. Hibbs, D. E.; Hursthouse, M. B.; Jones, I. G.; Jones, W.; Malik, K. M. A.; North, M. *J. Org. Chem.* **1998**, *63*, 1496. Jones, I. G.; Jones, W.; North, M. *J. Org. Chem.* **1998**, *63*, 1505. Ranganathan, D.; Haridas, V.; Kurur, S.; Thomas, A.; Madhusudanan, K. P.; Nagaraj, R.; Kunwar, A. C.; Sarma, A. V. S.; Karle, I. L. *J. Am. Chem. Soc.* **1998**, *120*, 8448.
(8) Chothia, C. *J. Mol. Biol.* **1973**, *75*, 295. Salemme, F. R. *Prog. Biophys. Mol. Biol.* **1983**, *42*, 95.
(9) (a) Haque, T. S.; Little, J. C.; Gellman, S. H. *J. Am. Chem. Soc.* **1994**, *116*, 4105. (b) Awasthi, S. K.; Raghothama, S.; Balaram, P. *Biochem. Biophys. Res. Commun.* **1995**, *216*, 375. (c) Haque, T. S.; Little, J. C.; Gellman, S. H. *J. Am. Chem. Soc.* **1996**, *118*, 6975. (d) Karle, I. L.; Awasthi, S. K.; Balaram, P. *Proc. Natl. Acad. Sci. U.S.A.* **1996**, *93*, 8189. (e) Raghothama, S. R.; Awasthi, S. K.; Balaram, P. *J. Chem. Soc., Perkin Trans. 2*, **1998**, 137.
(10) Haque, T. S.; Gellman, S. H. *J. Am. Chem. Soc.* **1997**, *119*, 2303. Stanger, H. E.; Gellman, S. H. *J. Am. Chem. Soc.* **1998**, *120*, 4236. Schenck, H. L.; Gellman, S. H. *J. Am. Chem. Soc.* **1998**, *120*, 4869.
(11) Rose, G. D.; Gierasch, L. M.; Smith, J. A. *Adv. Protein Chem.* **1985**, *37*, 1.
(12) Soth, M. J.; Nowick, J. S. *J. Org. Chem.* **1999**, *64*, 276.

10.1021/ja9929483 CCC: $19.00
Published on Web 05/24/2000

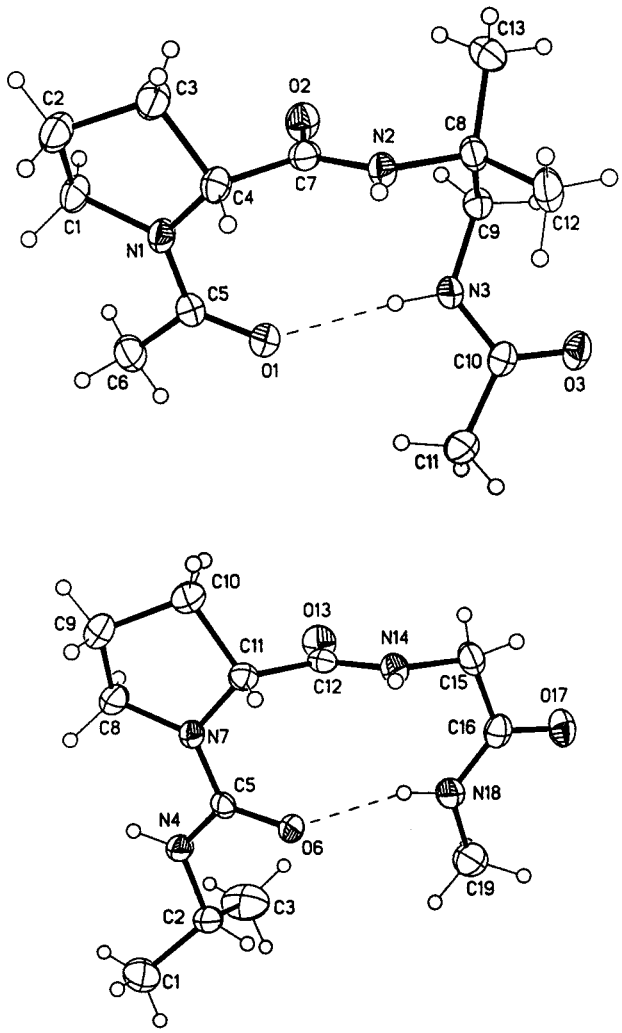

Figure 1. Solid state conformations of **1** (upper) and **2** (lower). Hydrogen bonds are shown as dotted lines.

peptide strand to a rigid strand mimic in an antiparallel sheet model.[13] (Nowick et al. have made extensive use of urea-based templates for creation of parallel β-sheet mimics.[3]) The crystal structures of **1** and **2** (Figure 1) show that these molecules can form 10-membered ring C═O- -H−N hydrogen bonds analogous to those commonly observed in β-turns.[11] In both cases,

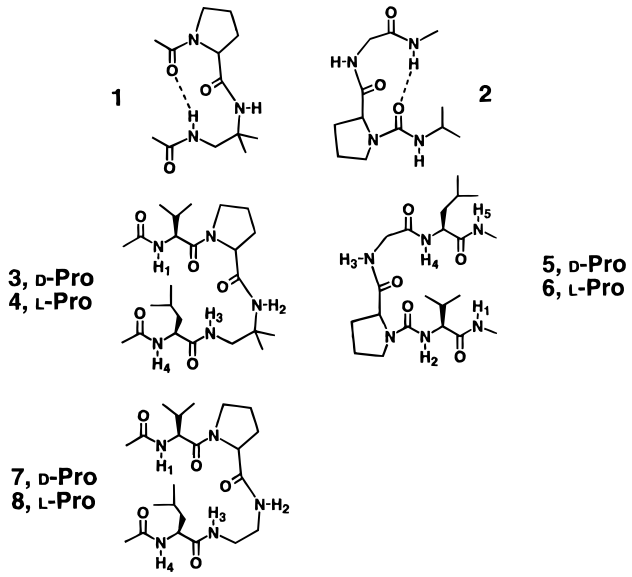

the intramolecular hydrogen bond displays a good geometry (for **1**, O- -H distance = 2.11 Å and N−H- -O angle = 175.4°; for **2**, O- -H distance = 2.02 Å and N−H- -O angle = 160.5°). These C═O- -H−N interactions would be the innermost of the interstrand hydrogen bonds if the core unit of **1** and/or **2** nucleated a two-stranded parallel sheet.

We examined tetrapeptide analogues **3**−**6**, each of which contains core unit **1** or **2**, to probe for parallel hairpin formation. We also examined **7** and **8**, which are related to **3** and **4** but lack the *gem*-dimethyl substitution on the core segment. In diastereomers **3** and **4**, a central unit corresponding to **1** connects L-valine and L-leucine strand residues via their C-termini. These molecules could form a minimal parallel sheet (one residue in each strand) if a hydrogen bond occurred between NH-1 and the acetyl C═O adjacent to Leu, in addition to the 10-membered ring hydrogen bond between NH-3 and Val C═O observed for **1**. Comparing the D-Pro and L-Pro diastereomers (**3** and **4**, respectively) allows us to determine whether the local twist of the linker influences parallel hairpin formation. The comparison was conducted in chloroform, a relatively nonpolar environment in which intramolecular hydrogen bonding provides a modest but not overwhelming driving force for folding.[9a,c,14]

The amide NH NMR chemical shifts (δNH) for **3** and **4** in a non-hydrogen bonding solvent like $CDCl_3$ provide insight on intramolecular hydrogen bonding patterns.[9a,c,14] δNH values are very sensitive to hydrogen bond formation, which typically causes a downfield shift of 2−3 ppm. For small oligoamides such as **3** and **4**, equilibration among non-hydrogen bonded and hydrogen bonded states is usually rapid on the NMR time scale, and the observed δNH values therefore reflect population-weighted averaging. Interpretation of δNH data in terms of intramolecular hydrogen bonding requires that the molecule of interest be sufficiently dilute to prevent hydrogen bond-mediated aggregation. Examination of δNH values as a function of the logarithm of solute concentration indicates that aggregation of **3**−**8** occurs above 10 mM; representative data for **3** are shown in Figure 2.

Table 1 contains δNH values measured at room temperature with 1 mM $CDCl_3$ solutions (nonaggregating conditions). For L-Pro diastereomer **4**, we observed multiple resonances for each proton, indicating the presence of slowly interconverting species, as is common for molecules that contain tertiary amides.[15] The δNH values given in Table 1 for **4** arise from the major rotamer of **4**. Only a single tertiary amide rotamer was detected for **3**. Among the four amide protons, only NH-1 shows a large difference ($\Delta\delta$NH = 1.9 ppm) between **3** and **4**. These data suggest that NH-1 is internally hydrogen bonded to a large extent in D-Pro diastereomer **3**, but that there is little or no hydrogen bonding at NH-1 in **4**. The other three amide protons vary by <0.3 ppm between the two diastereomers. The δNH-3 values (7.3 to 7.5 ppm) suggest that the 10-membered ring hydrogen bond is highly populated in both isomers.[9a,c,14] The δNH-2 and δNH-4 values (5.8 to 6.4 ppm) indicate that neither of these amide protons experiences much intramolecular hydrogen bonding in either isomer. Overall, the δNH data are consistent with our hypothesis that the D-Pro linker of **3** promotes parallel

(13) Kemp, D. S.; Bowen, B. R.; Muendel, C. C. *J. Org. Chem.* **1990**, *55*, 4650.

(14) Leading references on analysis of intramolecular hydrogen bonding in small amides and related compounds in organic solvents: Gellman, S. H.; Dado, G. P.; Liang, G.-B.; Adams, B. R. *J. Am. Chem. Soc.* **1991**, *113*, 1164. Tsang, K. Y.; Diaz, H.; Graciani, N.; Kelly, J. W. *J. Am. Chem. Soc.* **1994**, *116*, 3988. Nowick, J. S.; Abdi, M.; Bellamo, K. A.; Love, J. A.; Martinez, E. J.; Noronha, G.; Smith, E. M.; Ziller, J. W. *J. Am. Chem. Soc.* **1995**, *117*, 89. Gung, B. W.; Zhu, Z. *J. Org. Chem.* **1996**, *61*, 6482.

(15) Stewart, W. E.; Siddall, T. H. *Chem. Rev.* **1970**, *70*, 517.

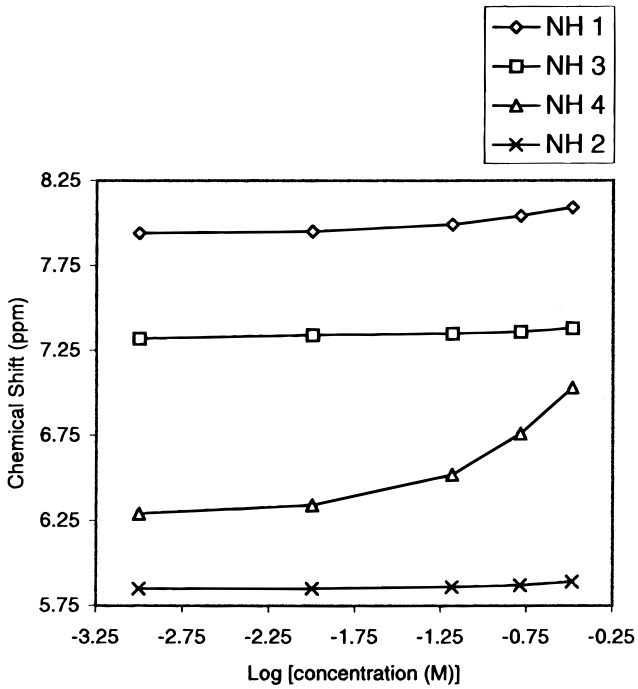

Figure 2. Amide proton NMR chemical shifts in $CDCl_3$ at room temperature, as a function of the logarithm of solute concentration, for the four NH groups of **3**.

Table 1. δ Data for **3**−**8**[a]

molecule	δNH-1	δNH-2	δNH-3	δNH-4	δNH-5
3	7.94	5.85	7.32	6.29	
4[b]	6.02	6.12	7.51	6.40	
5	7.30	5.24	6.30	8.40	6.70
6	6.65	5.03	7.48	7.76	6.38
7	8.00	6.89	7.20	6.24	
8[c]	6.74	6.64	7.36	6.06	

[a] Amide proton NMR chemical shifts measured in $CDCl_3$ at room temperature, with 1 mM solutions. [b] Major rotamer ca. 75% of a three-rotamer mixture. [c] Major rotamer ca. 85% of a two-rotamer mixture.

β-sheet interactions between the Val and Leu residues, while the L-Pro linker of **4** does not.

NOESY[16] data for **3** and **4** support our conclusion that only **3** has a significant population of the parallel hairpin conformation in $CDCl_3$. There are no NOEs involving nonadjacent residues in the NOESY spectrum of **4**. In contrast, **3** displays an NOE between Val NH and Leu $C_\alpha H$ (Figures 3 and 4), which is characteristic of a parallel sheet interaction between these two residues in which the valine residue provides the hydrogen bonding groups.[17,18] An NOE between Val $C_\alpha H$ and Pro $C_\delta H$ of **3** (not shown) confirms the *Z* configuration of the Val-Pro peptide bond. No NOEs inconsistent with the proposed hairpin conformation were observed for **3**.

Compounds **7** and **8** display δNH patterns that are similar to those observed for **3** and **4** (Table 1). In particular, the most significant difference between **7** and **8** involves NH-1, with D-Pro isomer **7** showing a greater degree of internal hydrogen bonding at NH-1 than L-Pro isomer **8**. The difference in δNH-1

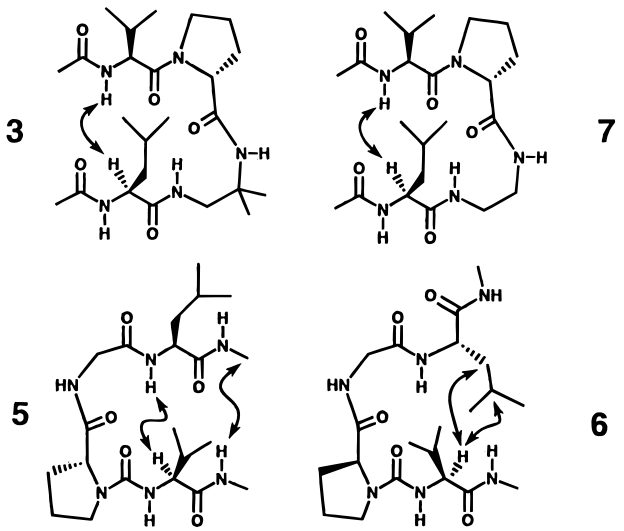

Figure 3. Summary of NOEs observed between protons on nonadjacent residues in **3**, **5**, **6**, and **7** in $CDCl_3$ (10 mM solutions; 24 °C). Resonance assignments were derived from COSY and NOESY (sequential NOE) data. NOESY mixing times (500 ms for **3**, 420 ms for **5**, 340 ms for **6**, 500 ms for **7**) were chosen based on T_1 measurements.

is consistent with more extensive parallel hairpin formation in **7** than in **8**. This conclusion is supported by observation of an NOE between Val NH and Leu $C_\alpha H$ of **7** but not **8** (Figure 3); **8** displays no NOEs between nonadjacent residues.

There is one significant difference between the diastereomeric pairs **3**/**4** and **7**/**8** in terms of δNH data: NH-2 is significantly further downfield in the latter pair relative to the former pair. Partial hydrogen bonding at NH-2 is not consistent with hairpin formation. The δNH-2 data suggest that the C-to-C linker lacking *gem*-dimethyl substitution (as in **7** and **8**) may be less effective at enforcing a β-turn-like conformation than the linker containing *gem*-dimethyl substitution (as in **3** and **4**).

NMR data for N-to-N linked tetrapeptide analogues **5** and **6**, which contain a central unit corresponding to **2**, indicate that hairpin formation is more favorable for D-Pro isomer **5** than for L-Pro isomer **6**. δNH data are presented in Table 1. NH-4 is the farthest downfield for each diastereomer, suggesting that the 10-membered ring hydrogen bond is highly populated in both cases.[9a,c,14] Parallel hairpin formation would involve hydrogen bonding at NH-1. This resonance is indeed significantly further downfield for **5** than for **6**, but the difference between the two δNH-1 values is smaller than observed for δNH-1 in **3** vs **4**. Interestingly, δNH-3 of the L-Pro isomer **6** suggests significant hydrogen bonding at this proton, which is not consistent hairpin formation. In contrast, δNH-3 of **5** suggests little intramolecular hydrogen bonding at this amide proton, as expected for the parallel hairpin conformation.

NOESY data strongly support our conclusion that D-Pro isomer **5** displays significant population of the parallel hairpin conformation in solution (Figures 3 and 4). Both of the $C_\alpha H$- -NH NOEs expected for a parallel sheet conformation[17] are observed for **5**: between NH-1 and the methyl group adjacent to NH-5, and between Val $C_\alpha H$ and NH-4. No NOEs inconsistent with the hairpin conformation are observed for **5**. L-Pro diastereomer **6** displays two interstrand NOEs, between $C_\alpha H$ of Val and side chain protons of Leu ($C_\beta H$ and $C_\gamma H$). Since the δNH-4 value suggests that there is considerable 10-membered ring hydrogen bonding in **6**, it is not surprising that some portion of the Val and Leu residues spend enough time in proximity to give rise to NOEs. The absence of the characteristic $C_\alpha H$- -NH

(16) Macura, S.; Ernst, R. R. *Mol. Phys.* **1980**, *41*, 95.

(17) Wüthrich, K. *NMR of Proteins and Nucleic Acids*; Wiley: New York, 1986.

(18) Nowick et al. have observed characteristic interstrand $C_\alpha H$- -$C_\beta H$ NOEs in their parallel β-sheet model systems (ref 3c and literature cited therein). Such NOEs, e.g., Leu-$C_\alpha H$- -Val-$C_\beta H$ in **3** and Val-$C_\alpha H$- -Leu-$C_\beta H$ in **5**, may be present in the NOESY spectra, but definitive identification is impossible because of resonance overlap.

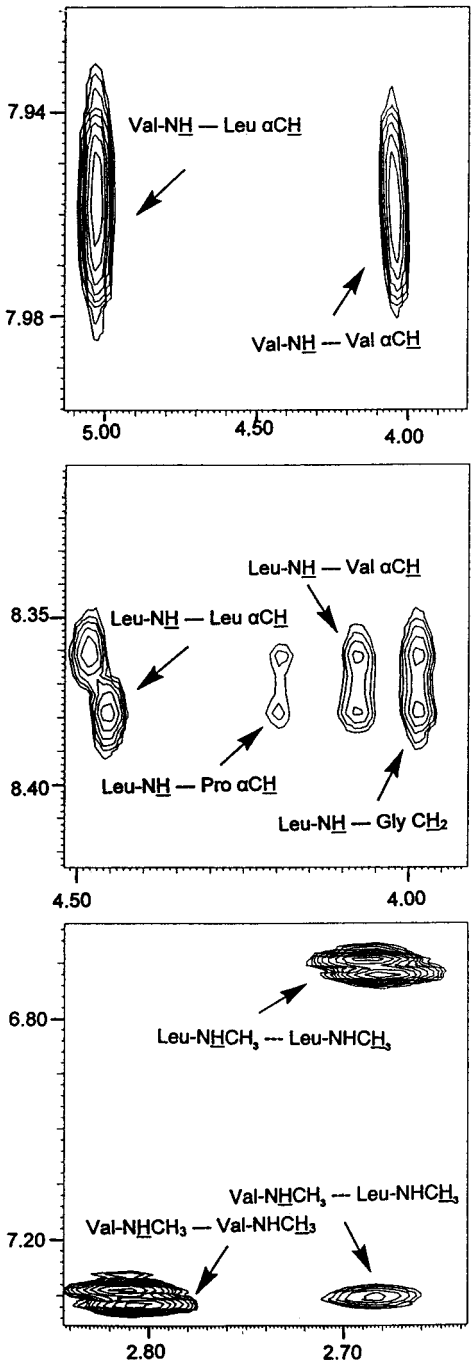

Figure 4. Representative NOESY data for **3** (uppermost panel) and **5** (lower two panels). Conditions are given in the caption to Figure 3.

NOEs, however, indicates that there is little or no parallel sheet interaction between the Val and Leu residues in **6**.

The results obtained in these parallel β-sheet model studies are complementary to previous findings that demonstrated that D-Pro-Xxx dipeptide segments strongly promote *antiparallel* β-sheet interactions between attached L-residue strands, while L-Pro-Xxx dipeptide segments strongly discourage antiparallel β-sheet interactions.[9,10] The antiparallel β-sheet model studies were inspired by statistical surveys of β-hairpins in crystalline proteins. Sibanda and Thornton showed that an unusual class of β-turns (types I′ and II′) occurs very commonly in β-hairpin loops,[19] and they rationalized this trend by noting that only type I′ and II′ β-turns have a local twist that is compatible with the right-handed twist of the strands.[8] We initially demonstrated proline configuration-based control of β-hairpin formation by examining tetrapeptides and tetrapeptide analogues in organic solvents;[9a,c] analogous behavior was subsequently documented for longer peptides in aqueous solution.[10] It therefore seems likely that using D-Pro-containing units corresponding to **1** and **2** to link longer L-residue strands will lead to well-defined parallel sheet model systems in aqueous solution.

Conclusions. We have shown that the folding of minimal parallel β-sheet model systems can be controlled by manipulating the local conformational preference of the segment used to connect the strand residues. Establishing linker-based control of parallel sheet folding is important: use of proline configuration as an "on/off switch" has proven to be extremely valuable in antiparallel β-sheet model studies because the "off" state provides a crucial negative control.[10] Most of the parallel linkers reported to date are locally achiral, which means that they have no preferred twist.[3,4,6] This study is the first to probe the relationship between linker twist and parallel sheet formation.

Experimental Section

NMR Spectroscopy. One-dimensional spectra for aggregation studies were obtained on either a Bruker AC-300 or a Varian Unity 500 spectrometer. Samples were prepared by serial dilution from the most concentrated sample (ca. 100 mM). Samples were prepared on the benchtop using dry $CDCl_3$. Two-dimensional spectra for conformational analysis were obtained on either a Varian Unity-500 or Varian Inova-500 spectrometer. Samples used for conformational analysis were prepared on the benchtop and were typically between 5 and 10 mM. Proton signals were assigned via COSY spectra. Data for conformational analysis came from NOESY spectra with typical mixing times of 500−600 ms. All spectra were acquired using standard Varian pulse sequences and worked up using Varian VNMR software.

Synthesis. Peptide bond formation was accomplished via standard solution-phase procedures, with dicyclohexylcarbodiimide and *N*-hydroxysuccinimide.[20] The amino groups of 1,2-diaminoethane and 1,2-diamino-1,1-dimethylethane were orthogonally protected with *tert*-butyloxycarbonyl and benzyloxycarbonyl groups. Monoprotection of these diamines was accomplished by slow addition of di(*tert*-butyloxycarbonyl)dicarbonate or benzyl chloroformate to a 3- to 5-fold excess of the diamine; monoprotection of 1,2-diamino-1,1-dimethylethane occurred selectively at the 2-amino group. Urea bond formation involved triphosgene methodology,[21] e.g., formation of the isocyanate of leucine benzyl ester, followed by reaction with a proline derivative. When the proline nitrogen was incorporated into a urea group, subsequent amide bond formation at the proline carbonyl led to extensive epimerization at the proline α-carbon; however, urea−prolyl bonds could be formed without epimerization after the proline carbonyl had been coupled to an amine.

Characterization. Final compounds were characterized by ^{1}H and ^{13}C NMR and high-resolution mass spectroscopy. ^{1}H NMR spectra were referenced to TMS, ^{13}C NMR spectra to $CDCl_3$. DEPT 90 and 135 were used to identify proton multiplicity of carbons. Spectra reported for characterization were obtained on a Bruker Ac-300 spectrometer.

Ac-Pro-2MDAP-Ac (1). ^{1}H NMR ($CDCl_3$, 300 MHz) δ 1.24 (s, 3 H), 1.34 (s, 3 H), 1.97 (m, 2 H), 2.04 (s, 3 H), 2.10 (m, 2 H), 2.12 (s, 3 H), 3.48 (m, 3 H), 3.67 (m, 1 H), 4.21(m, 1 H), 6.74 (s, 1 H), 7.33 (t, J = 6.0 Hz, 1 H). ^{13}C NMR (CDC_3, 75.5 MHz) δ 22.50 (CH3), 22.83 (CH3), 24.26 (CH3), 24.80(CH2), 25.07 (CH3), 29.08 (CH2), 46.61 (CH2), 48.24 (CH2), 54.54 (C), 60.89 (CH), 170.19 (CO), 171.15 (CO), 171.77 (CO). EI-MS *m*/*z* calculated 269.1739, observed 269.1760.

^{i}PrNH-urea-Pro-Gly-NHMe (2). ^{1}H NMR ($CDCl_3$, 300 MHz) δ 1.17 (d, J = 3.7 Hz, 3 H), 1.19 (d, J = 3.7 Hz 3 H), 2.08 (m, 4 H),

(19) Sibanda, B. L.; Thornton, J. M. *Nature* **1985**, *316*, 170. Gunasekaran, K.; Ramakrishnan, F.; Balaram, P. *Protein Eng.* **1997**, *10*, 1131.

(20) Bodanszky, M.; Bodanszky, A. *The Practice of Peptide Synthesis*; Springer-Verlag: New York, 1984.

(21) (a) Nowick, J. S.; Holmes, D. L.; Noronha, G.; Smith, E. M.; Nguyen, T. M.; Huang, S. L. *J. Org. Chem.* **1996**, *61*, 3929. (b) Majer, P.; Randad, R. S. *J. Org. Chem.* **1994**, *59*, 1937.

2.78 (d, $J = 4.71$ Hz, 3 H), 3.27 (m, 1 H), 3.39 (m, 1 H), 3.95 (m, 3 H), 4.29 (dd, $J = 7.89$, 3.79, 1 H), 4.33 (d, $J = 7.6$, 1 H), 7.00 (t, $J = 6.3$, 1 H), 7.36 (q, $J = 4.7$ Hz, 1 H). ^{13}C NMR (CDC_{l3}, 75.5 MHz) δ 23.26 (CH3), 23.41 (CH3), 25.13 (CH2), 28.98 (CH3), 42.76 (CH), 43.08 (CH2), 46.27 (CH2), 61.07 (CH), 157.19 (CO), 170.18 (CO), 173.68 (CO). EI-MS *m*/*z* calculated 270.1692, observed 270.1668.

Ac-Val-D-Pro-2MDAP-Leu-Ac (3). ^{1}H NMR ($CDCl_3$, 300 MHz) δ 0.92 (d, $J = 5.7$ Hz, 3 H), 0.94 (d, $J = 2.5$ Hz, 3 H), 0.98 (d, $J = 6.3$ Hz, 3 H), 1.02 (s, 3H), 1.11 (d, $J = 6.6$ Hz, 3 H), 1.40 (s, 3H), 1.41 (m, 1 H), 1.53 (m, 2 H), 1.62 (m, 1 H), 1.81 (s, 3 H), 2.00 (m, 2 H), 2.03 (s, 3 H), 2.25 (m, 2 H), 3.12 (q, $J = 7.3$ Hz, 1 H), 3.52 (dd, $J = 13.3$, 9.8, 1 H), 3.59 (dd, $J = 13.3$, 2.1 Hz, 1 H), 4.06 (dd, $J = 10.0$, 6.3 Hz, 1 H), 4.27 (dd, $J = 8.5$, 4.3, 1 H), 4.36 (m, 1 H), 5.01 (dt, $J = 9.5$, 5.5 Hz, 1 H), 5.88 (s, 1 H), 6.70 (d, $J = 9.4$ Hz, 1H), 7.37 (dd, $J = 9.4$, 1.8 Hz, 1 H), 8.03 (d, $J = 6.2$ Hz, 1H). ^{13}C NMR (CDC_{l3}, 75.5 MHz) δ 18.93 (CH3), 19.29 (CH3), 21.71 (CH3), 21.97 (CH3), 23.15 (CH3), 23.45 (CH3), 24.70 (CH), 24.82 (CH2), 25.19 (CH3), 29.46 (CH), 29.65 (CH2), 44.05 (CH2), 45.50 (CH2), 48.027 (CH2), 50.98 (CH), 53.92 (C), 58.71 (CH), 62.20 (CH), 170.14 (CO), 171.17 (CO), 171.92 (CO), 172.65 (CO), 172.79 (CO). EI-MS *m*/*z* calculated 481.3342, observed 481.3313.

Ac-Val-L-Pro-2MDAP-Leu-Ac (4). ^{1}H NMR ($CDCl_3$, 300 MHz) δ 0.92 (d, $J = 5.7$ Hz, 3 H), 0.94 (d, $J = 2.5$ Hz, 3 H), 0.98 (d, $J = 6.3$ Hz, 3 H), 1.02 (s, 3H), 1.11 (d, $J = 6.6$ Hz, 3 H), 1.40 (s, 3H), 1.41 (m, 1 H), 1.53 (m, 2 H), 1.62 (m, 1 H), 1.81 (s, 3 H), 2.00 (m, 2 H), 2.03 (s, 3 H), 2.25 (m, 2 H), 3.12 (q, $J = 7.3$ Hz, 1 H), 3.52 (dd, $J = 13.3$, 9.8, 1 H), 3.59 (dd, $J = 13.3$, 2.09 Hz, 1 H), 4.06 (dd, $J = 10.0$, 6.3 Hz, 1 H), 4.27 (dd, $J = 8.5$, 4.3, 1 H), 4.36 (m, 1 H), 5.01 (dt, $J = 9.5$, 5.5 Hz, 1 H), 5.88 (s, 1 H), 6.70 (d, $J = 9.4$ Hz, 1H), 7.37 (dd, $J = 9.4$, 1.8 Hz, 1 H), 8.03 (d, $J = 6.2$ Hz, 1H). ^{13}C NMR (CDC_{l3}, 75.5 MHz) δ 17.78 (CH3), 19.12 (CH3), 22.46 (CH3), 22.90 (CH3), 23.07 (CH3), 23.16 (CH3), 24.27 (CH3), 24.76 (CH), 25.23 (CH2), 26.32 (CH3), 28.92 (CH2), 31.68 (CH), 41.53 (CH2), 45.50 (CH2), 48.12 (CH2), 52.21 (CH), 54.90 (CH), 55.40 (C), 61.50 (CH), 170.01 (CO), 170.29 (CO), 171.05 (CO), 172.52 (CO), 172.88 (CO). EI-MS *m*/*z* calculated 481.3342, observed 481.3262.

MeNH-Val-urea-D-Pro-Gly-Leu-NHMe (5). ^{1}H NMR ($CDCl_3$, 300 MHz) δ 0.91 (d, $J = 6.3$ Hz, 3 H), 0.93 (d, $J = 1.5$ Hz, 3 H), 0.98 (d, $J = 1.5$ Hz, 3 H), 0.96 (d, $J = 6.5$ Hz, 3 H), 1.73 (m, 3H), 1.94 (m, 1 H), 2.05 (m, 2 H), 2.20 (m, 2 H), 2.68 (d, $J = 4.8$ Hz, 3 H), 2.80 (d, $J = 4.7$ Hz, 3 H), 3.45 (m, 2 H), 3.98 (dd, $J = 6.7$, 1.2, 1 H), 4.07 (t, $J = 8.0$ Hz, 1 H), 4.20 (dd, $J = 7.5$, 5.8 Hz, 1 H), 4.46 (td, $J = 8.6$, 6.1, 1 H), 5.29 (d, $J = 8.4$ Hz, 1 H), 6.49 (t, $J = 6.4$ Hz, 1 H), 6.74 (q, $J = 4.7$ Hz, 1H), 7.35 (q, $J = 4.6$ Hz, 1 H), 8.38 (d, $J = 8.4$ Hz, 1H). ^{13}C NMR (CDC_{l3}, 75.5 MHz) δ 18.59 (CH3), 19.04 (CH3), 21.84 (CH3), 24.65 (CH), 25.12 (CH3), 25.87 (CH3), 26.00 (CH3), 29.36 (CH2), 32.35 (CH), 38.14 (CH2), 43.01 (CH2), 45.98 (CH2), 51.09 (CH), 59.96 (CH), 61.52 (CH), 156.62 (CO), 169.63 (CO), 172.52 (CO), 172.92 (CO), 174.04 (CO). EI-MS *m*/*z* calculated 454.2904, observed 454.2914.

MeNH-Val-urea-L-Pro-Gly-Leu-NHMe (6). Major rotomer: ^{1}H NMR ($CDCl_3$, 300 MHz) δ 0.90 (d, $J = 4.5$ Hz, 3 H), 0.93 (d, $J = 4.5$ Hz, 3 H), 0.95 (d, $J = 6.6$ Hz, 3 H), 0.98 (d, $J = 6.6$ Hz, 3 H), 1.58 (m, 2H), 1.77 (m, 1 H), 2.00 (m, 2 H), 2.15 (m, 3 H), 2.78 (d, $J = 4.8$ Hz, 3 H), 2.83 (d, $J = 4.8$ Hz, 3 H), 3.39 (m, 1 H), 3.51 (m, 1 H), 3.77 (dd, $J = 17.1$, 5.0, 1 H), 3.91 (t, $J = 8.4$ Hz, 1 H), 4.14 (m, 2 H), 4.50 (td, $J = 8.7$, 6.0, 1 H), 5.13 (d, $J = 8.4$ Hz, 1 H), 6.49 (q, $J = 2.7$ Hz, 1 H), 6.80 (m, 2H), 7.78 (d, $J = 8.4$ Hz, 1 H). ^{13}C NMR (CDC_{l3}, 75.5 MHz) δ 18.93 (CH3), 19.34 (CH3), 21.90 (CH3), 22.99 (CH3), 24.72 (CH), 25.32 (CH2), 26.16 (CH3), 26.25 (CH3), 29.48 (CH2), 30.51 (CH), 40.54 (CH2), 43.21 (CH2), 46.30 (CH2), 51.72 (CH), 60.58 (CH), 61.17 (CH), 157.15 (CO), 169.65 (CO), 172.78 (CO), 173.23 (CO), 173.74 (CO). EI-MS *m*/*z* calculated 454.2904, observed 454.2897.

Ac-Val-D-Pro-EDA-Leu-Ac (7). ^{1}H NMR ($CDCl_3$, 300 MHz) δ 0.93 (d, $J = 6.4$ Hz, 3 H), 0.96 (d, $J = 6.2$ Hz, 3 H), 0.98 (d, $J = 6.7$ Hz, 3 H), 1.14 (d, $J = 6.6$ Hz, 3 H), 1.60 (m, 3 H), 1.79 (s, 3 H), 2.02 (m, 2 H), 2.04 (s, 3 H), 2.83 (m, 1 H), 3.50 (m, 2 H), 3.57 (dd, $J = 7.5$, 2.1 Hz, 1 H), 3.64 (m, 1 H), 3.98 (dd, $J = 9.9$, 5.5 Hz, 1 H), 4.29 (ddd, $J = 9.9$, 6.8, 5.1 Hz, 1 H), 4.46 (dd, $J = 8.7$, 3.7 Hz, 1 H), 4.92 (m, 1 H), 6.39 (d, $J = 10.2$ Hz, 1 H), 6.90 (dd, $J = 6.6$, 4.8 Hz, 1 H), 7.22 (bt, 1 H), 8.03 (d, $J = 5.7$ Hz, 1 H). ^{13}C NMR (CDC_{l3}, 75.5 MHz) δ 19.00 (CH3), 19.42 (CH3), 21.61, 21.89 (CH3), 23.14, 23.41 (CH3), 24.55 (CH2), 24.77 (CH), 29.38 (CH2), 29.38 (CH), 36.38 (CH2), 39.01 (CH2), 43.22 (CH2), 47.90 (CH2), 51.08 (CH), 59.30 (CH), 61.80 (CH), 170.57 (CO), 171.78 (CO), 172.92 (CO), 173.11 (CO), 173.44 (CO). EI-MS *m*/*z* calculated 453.2951, observed 453.2953.

Ac-Val-L-Pro-EDA-Leu-Ac (8). ^{1}H NMR ($CDCl_3$, 300 MHz) δ 0.94 (d, $J = 2.1$ Hz, 3 H), 0.96 (d, $J = 2.7$ Hz, 3 H), 0.97 (d, $J = 6.6$ Hz, 3 H), 1.01 (d, $J = 6.6$ Hz, 3 H), 1.65 (m, 4 H), 2.00 (s, 3 H), 2.02 (s, 3 H), 2.13 (m, 4 H), 3.10 (m, 2 H), 3.30 (m, 1 H), 3.67 (m, 1 H), 3.88 (m, 1 H), 4.21 (t, $J = 7.0$ Hz, 1 H), 4.54 (m, 1 H), 4.64 (dd, $J = 9.0$, 7.5 Hz, 1 H), 6.12 (d, $J = 7.7$ Hz, 1 H), 6.71 (m, 2 H), 6.90 (dd, $J = 4.9$, 4.6 Hz, 1 H). ^{13}C NMR (CDC_{l3}, 75.5 MHz) δ 18.05 (CH3), 19.06 (CH3), 22.44 (CH3), 22.64 (CH3), 22.95 (CH3), 23.08 (CH3), 24.74 (CH), 25.23 (CH2), 28.88 (CH2), 31.48 (CH), 38.34 (CH2), 38.88 (CH2), 41.25 (CH2), 48.03 (CH2), 52.30 (CH), 55.66 (CH), 61.02 (CH), 170.20 (CO), 170.56 (CO), 171.60 (CO), 172.32 (CO), 173.29 (CO). EI-MS *m*/*z* calculated 453.2951, observed 453.2938.

Acknowledgment. This research was supported by the National Science Foundation (CHE-9820952). J.D.F. was supported in part by a National Research Service Award (T32 GM08923). NMR spectrometers were purchased in part with funds from the NIH (S10 RR04981). We thank Prof. James S. Nowick for helpful comments.

Supporting Information Available: Crystallographic data for **1** and **2** and δNH values as a function of concentration for **3**−**6** (PDF). This material is available free of charge via the Internet at http://pubs.acs.org.

JA9929483